TiS Trends in Sciences
TRENDS IN SCIENCES 2027; 24(1): 14471
SPRINT Scholarly Publishing and Repository Integration Center
https://doi.org/10.48048/tis.2027.14471
RESEARCH ARTICLE

Cellular Development and Ultrastructural Characteristics of *Halymenia durvillei* Bory de Saint-Vincent, 1828

Yupadee Paopun[1,*], Piyanan Thanomchat[1], Siriphan Sukkhaeng[2], Chanram Roopkham[1], Nustsaba Kronburee[1], Yanisa Detpakdee[1], Nuttha Sanevas[3], Prapat Kosawatpat[4] and Naratorn Chumnum[4]

[1]*Scientific Equipment and Research Division, Kasetsart University Research and Development Institute, Kasetsart University, Bangkok 10900, Thailand*
[2]*Central Laboratory and Greenhouse Complex, Research and Academic Service Center, Faculty of Agriculture at Kamphaeng Saen, Kasetsart University, Kamphaeng Saen Campus, Nakhon Pathom 73140, Thailand*
[3]*Department of Botany, Faculty of Science, Kasetsart University, Bangkok 10900, Thailand*
[4]*Phetchaburi Coastal Aquaculture Research and Development Center, Coastal Aquaculture Research and Development Division, Department of Fisheries, Phetchaburi 76100, Thailand*

([*]Corresponding author's e-mail: rdiydp@ku.ac.th)

Received: 21 May 2026, Revised: 4 July 2026, Accepted: 14 July 2026, Published: 10 September 2026

Abstract

Halymenia durvillei Bory de Saint-Vincent, 1828 is a marine red alga with potential relevance for aquaculture and biomass production. Samples were collected from a Coastal Aquaculture Research Center in Thailand, and cultivated in culture tanks with natural seawater for up to 3 months. This study examined the morphological and ultrastructural changes in *H. durvillei* thalli across different cultivation periods to assess developmental progression and determine an optimal harvest time for the most mature growth stage to maximize biomass production. Molecular identification based on the *rbcL* gene sequencing confirmed the taxonomic identity of the studied alga, showing 99% sequence similarity to *H. durvillei.* Light microscopy (LM) and transmission electron microscopy (TEM) revealed progressive increases in thallus thickness and pronounced changes in cellular organization with increasing cultivation period. Cell size increased markedly, and the differences in outer cortical cells became significantly apparent with cultivation time. Each cell contained a single large chloroplast with well-developed thylakoids, phycobilisomes, pyrenoids, and plastoglobules. In addition, floridean starch granules and lipid droplets were observed in the cytoplasm and increased with the cultivation period. These ultrastructural changes indicate enhanced development of chloroplast-associated storage systems, reflecting increased accumulation of carbohydrate and lipid reserves. After 3 months of cultivation, thalli exhibited the largest cell size and the most pronounced development of chloroplast-associated storage structures, suggesting advanced plastid maturation and metabolic readiness. Overall, a cultivation period of approximately 3 months was optimal for obtaining mature thalli with enhanced storage capacity. *H. durvillei* is a high-value red seaweed with broad potential applications in the food, pharmaceutical, and biotechnological industries.

Keywords: *Halymenia durvillei*, Red algae, Cellular, Ultrastructure, Chloroplast, Phycobilisome, Development

Introduction

Dragon's tongue red macroalgae (*Halymenia durvillei* Bory de Saint-Vincent, 1828) is a member of the family Halymeniaceae, established by Bory in 1828. It is distributed in the Indian Ocean, Indochina, New Guinea, the Pacific Ocean, Japan, the China Sea, the Philippines, Australia [1], Indonesia, Singapore, Malaysia, and Thailand [2]. This species occurs on the

outer reef wall and within reef passes at depths of 10 - 40 m [3].

The thallus of the *H. durvillei* is erect, firmly gelatinous, and slippery. It can be up to 42 cm long and about 5.4 cm wide. The thallus exhibits colors ranging from pink to red [3,4]. The anatomical characteristic of the thallus consists of a cortex that is divided into the outer cortex of 2 - 4 cell layers and the inner cortex of about 3 - 6 cell layers. The outer cortex cells are subspherical to elongated, measuring 8 - 19 µm, while the inner cortex cells are spherical to stellate, measuring 11 - 25 µm. The medulla, located at the center of the thallus, ranges from 185 to 1,250 µm in thickness [4]. The medulla is composed of filamentous cells, 8 - 9 µm in diameter. The morphology of the *H. durvillei* thallus exhibits considerable variety depending on thallus length [5]. In Japan, the Philippines, and Thailand, the thallus typically measures 17 - 18 cm long. In Indonesia, however, it can reach approximately 24 cm. In Malaysia, it can grow up to 50 cm. Furthermore, thallus branching patterns can be classified as dichotomous, sub-dichotomous, and trichotomous. The thallus of *H. durvillei* demonstrated morphological variation when grown under different environmental conditions [5]. Blade branching patterns varied, including pinnate, distichous, dichotomous, and sub-dichotomous types. For this reason, accurate species identification of *Halyminia* requires a combination of morphological characteristics and molecular markers. Red algal cells are eukaryotic and consist of a cell wall, cytoplasm, and membrane-bound organelles, including chloroplasts, mitochondria, and vacuoles. Their chloroplasts contain phycobilisomes, which are characteristic of Rhodophyta [6].

DNA is the genetic material of living organisms. Analysis of short DNA strands from chromosomal segments revealed pronounced differences between species but low variability within the same species. DNA barcodes are used to identify organisms (according to the Consortium for the Barcoding of Life, CBOL; http://barcoding.si.edu/) [7]. In red algae, DNA barcoding of the *rbcL* gene was performed together with morphological analysis to classify the species. Therefore, the *rbcL* gene was used as the standard marker to identify red algae [8-13].

Previous studies on the genus *Halymenia* have demonstrated that growth performance and pigment composition are strongly influenced by culture conditions, particularly light quality. For example, growth and pigment dynamics in *Halymenia floresii* were shown to vary significantly under different light qualities, indicating the close relationship between physiological growth responses and pigment composition in this genus [14]. Similarly, studies on other red algae have reported that light quality played a critical role in regulating growth and pigment content. In *Gracilaria birdiae,* variations in light quality significantly affected growth, reproduction, and pigment composition, further emphasizing the importance of light as a key environmental factor influencing physiological performance in red algae [15]. Additionally, the effects of light, water motion, and stocking density on the growth and pigment content of *H. durvillei* have been investigated under laboratory conditions [16]. However, these studies have primarily focused on physiological responses without any detailed information on cellular structural development during cultivation.

Given the high economic and biotechnological values of *H. durvillei*, a deeper understanding of its cellular and ultrastructural development during cultivation is essential. The thallus of *H. durvillei* is applied in the production of pharmaceuticals, agar, carrageenan, alginates, human food, fish meal, animal feed, and organic fertilizers [2]. The important bioactive compounds derived from red algae, such as phycobiliproteins, RuBisCO, peptides, sulfated galactans, carrageenan, lectins, and bromophenols, have been widely studied [17]. Moreover, marine red algae produce agarose, which is widely used for cellular encapsulation, as a growth medium for the immobilization of cells and enzymes, and as an electrophoresis substrate for pharmaceutical applications [18]. In addition to these applications, *H. durvillei* extracts possess various biological activities and have potential applications in biotechnology and pharmaceutical research [19]. Furthermore, these extracts have been reported to exhibit anticancer activity against glioblastoma cells [20].

Although previous studies have examined the growth, morphology, and cultivation of *H. durvillei*, knowledge of its cellular development and ultrastructural changes remains limited. Therefore, the present study provides new insights into these aspects,

which may contribute to maximizing biomass production and enhancing the yield of valuable bioactive compounds. The goals of this study are to investigate cellular and ultrastructural changes, including intracellular storage structures, during various cultivation periods.

Materials and methods

In this study, DNA extraction and purification from *Halymenia* seaweed were conducted to determine the genetic material. Morphological features were investigated using a light microscope (LM) and a transmission electron microscope (TEM). The thallus structures of *H. durvillei* at different culture periods were analyzed to measure cell size and cell density. This study laid the groundwork for further research to determine the optimal culture period for *H. durvillei* to produce bioactive compounds, which can be utilized at both community and industrial levels.

Preparation of *H. durvillei* thalli

Samples of *H. durvillei* were collected from the Phetchaburi Coastal Aquaculture Research and Development Center, Bang Kaeo Sub-District, Ban Laem District, Phetchaburi Province, Thailand (13.043677°N, 100.087064°E). *H. durvillei* was cultured in culture tanks measuring 5×4×1.5 m^3 (containing 25 m^3) filled with seawater at a salinity of 30 - 32 ppt. The wells were covered with a 60% light-intensity, slant-screen. Structural features of *H. durvillei* were analyzed at different culturing periods (0, 1, 2 and 3 months). At each sampling time, 10 thalli were randomly collected from the culture tanks for morphological and ultrastructural analyses. The experiments were conducted from July to October 2024.

DNA extraction and purification

Fresh thalli collected at the beginning of the experiment were used for DNA extraction and molecular identification. Genomic DNA was isolated from *H. durvillei* samples following the CTAB protocol of Doyle and Doyle (1987), using a buffer with the following composition: 100 mM Tris-HCl; 20 mM Na_2EDTA; 1.4 M NaCl; 2% (w/v) CTAB (pH 8.0), 0.5% 2-mercaptoethanol, and 1% PVP. The quality and quantity of the extracted DNA were assessed using a Nanophotometer ® NP80 (Implen, Germany).

Polymerase chain reaction (PCR) amplification and sequencing

Total genomic DNA was diluted at a final concentration of 50 ng/µL and used as a DNA template in PCR amplification. Primers targeting a region of the *rbcL* gene (F481 GTAGAACGTGAGCGTATGGA; R1150: GCATTTGTCCGCAGTGAATACC) were used for amplification [13].

The total PCR reaction volume was 50 µL, consisting of 10 µL DNA template, i-StarMAX II PCR Master Mix (iNtRON Biotechnology Inc., Seongnam, Korea), and 2.5 µL of each primer (10 pmol/µL). The final volume was adjusted to 50 µL with muclease-free water. PCR amplification was performed using a thermocycler (PCRmax® ALPHA 1, UK) under the following program: an initial denaturation at 94 °C for 4 min, followed by 35 cycles of denaturation at 94 °C for 30 s, annealing at 55 °C for 30 s, extension at 72 °C for 2 min, and a final extension at 72 °C for 5 min.

The amplified DNA fragments were separated on a 1.5% agarose gel containing 50 µg/mL ethidium bromide in 1X TAE buffer and visualized under UV light using a gel documentation system (UVITEC Imaging Systems, UK). A 100 bp DNA ladder (Solis Biodyne™, Estonia) was included to determine the fragment size. PCR products were analyzed by automated DNA sequencing using BTSeq™ (Barcode-Tagged Sequencing; CELEMICS, Seoul, Korea). The resulting sequences were compared with nucleotide sequences in the GenBank database using the BLAST (Basic Local Alignment Search Tool) program. For further information on GenBank and its sequence retrieval and analysis services, the NCBI homepage can be accessed at: http://www.ncbi.nlm.nih.gov [22].

Light Microscopy (LM) and Transmission Electron Microscopy (TEM)

H. durvillei thalli samples were examined using a compound light microscope (Leica: DM750) to observe the surface view. The cells were analyzed to determine cell size and cell density per 1,000 μm^2. For each cultivation period, 10 thalli were randomly collected for morphological and ultrastructural analyses. Cell size was determined by measuring 400 randomly selected cells. Cell density was quantified from 40 randomly selected observation fields, and thallus thickness was measured at 120 randomly selected positions. The

samples were prepared in transverse sections and observed by a compound light microscope and a transmission electron microscope (TEM). The samples were cut into 2×3 mm² pieces and prefixed overnight at 4 °C in 2.5% glutaraldehyde, which was prepared at 27 ppt salinity. They were post-fixed in 2% osmium tetroxide in distilled water for 2 h, dehydrated through an acetone series for 15 min per step, and then infiltrated and embedded in Spurr's resin [23-25]. The samples were sectioned into 500 nm-thick slices using a glass knife on an ultramicrotome (Leica: EM UC7), double-stained with 1% toluidine blue in distilled water mixed with 2.5% borax in distilled water at 85 °C [26], and post-stained with 1% basic fuchsin in distilled water [27,28]. The thick-section samples were examined under a compound light microscope (Zeiss: Axio Star Plus). The thin sections (100 nm) were double-stained with 5% uranyl acetate in 50% ethanol for 15 min and 1% lead citrate for 15 min. The sections were then examined under a TEM (Hitachi: HT7700) [29-31].

Statistical analysis

All experimental data are presented as mean ± standard deviation (SD). Measurements of outer cortical cell size, cell density, and thallus thickness were obtained from ten independent biological replicates for each cultivation period. Data were analyzed using one-way analysis of variance (ANOVA), followed by Duncan's Multiple Range Test (DMRT) for multiple comparisons at a significance level of $p < 0.05$. Statistical analyses were performed using IBM SPSS Statistics for Windows, Version 26.0 (IBM Corp., 2019).

Results and discussion

Molecular analysis of the DNA of the *Halymenia* seaweed

The molecular identification of a cultured red alga in Phetchaburi Province, Thailand, revealed that the *Halymenia* PCR products targeting the *rbcL* gene were amplified using specific primers and visualized by agarose gel electrophoresis. The apparent size of the PCR product was approximately 700 base pairs (**Figure 1**). The PCR products were sequenced and compared to 10 sequences in the GenBank database (analyzed on Jan 21, 2025). It was found that the sequence showed 99 % with the *H. durvillei*, as the following accession numbers: LT969719 99%, JX000240 98%, JX000238 98%, MW275903 98%, ON010713 98%, MW690956 98%, MW690957 98%, MK812821 98%, AY772020 98%, and JX000246 97%. All 10 *rbcL* gene sequences were aligned, and a phylogenetic tree was constructed, showing similarity to *H. durvillei* (**Figure 2**). The *rbcL* gene was sequenced to identify the sample species. Comparison with sequences in the GenBank database revealed 99% sequence identity with *H. durvillei* (accession number LT969719).

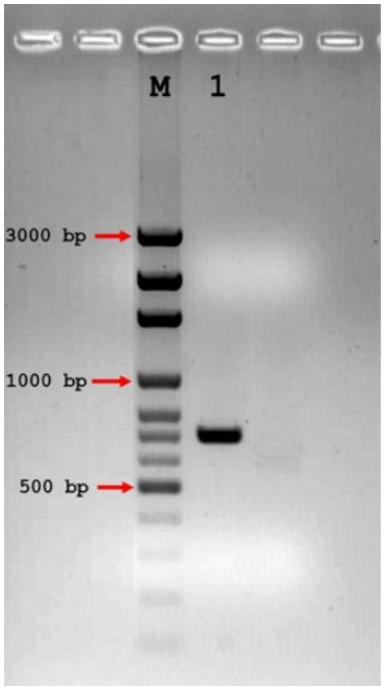


Figure 1 Agarose gel electrophoresis (1.5%) for PCR products using specific primers for the *rbcL* gene, showing a positive band at 700 bp. Lane M = marker 100 bp DNA ladder (Solis Biodyne TM, Estonia), Lane 1 = sample of *Halymenia* seaweed.

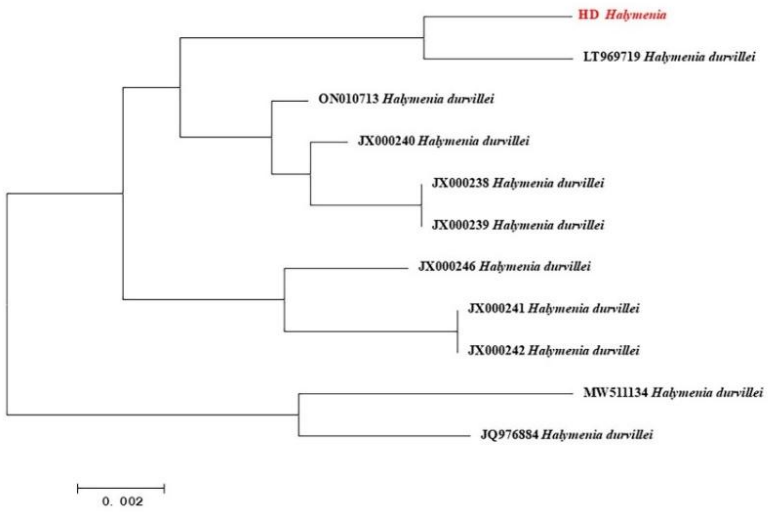


Figure 2 Phylogenetic tree using the neighbor-joining method based on nucleotide sequences of the *rbcL* gene.

Nucleotide analysis of the *rbcL* gene from Dragon's tongue red alga showed 99% sequence identity with *H. durvillei* (GenBank accession number LT969719). Ten sequences of nucleotides from similar *Halymenia* seaweed were analyzed, and a phylogenetic tree was constructed. The result confirmed that the alga in this study was *H. durvillei*. Analysis of the amplified *rbcL* gene using molecular markers confirmed that the samples belong to the red algae of the genus *Halymenia* [5,11,13,32-34].



Figure 3 Photograph of the thallus of *H. durvillei* showing external features. The thallus is irregularly branched with reddish coloration.

Comparative morphological and anatomical characters of the *H. durvillei* thallus at different culture periods

H. durvillei has red thalli, which can be smooth and branched thalli (**Figure 3**). The thallus surface revealed the organization of the outer cortex cells. The cells exhibited various shapes, including round, roundish, oval, and polygonal. The chloroplasts were positioned at the periphery of the cell (**Figures 4(A) - 4(D)**). Cell sizes varied over the culture period. As the culture times increased, the cells elongated to larger sizes. The data in **Table 1** indicated that the cells elongated up to 3 months. At 3 months of thallus culture, the cell size was larger than at 0, 1, and 2 months. Cell width increased from 7.38 ± 1.06 µm at 0 months to 9.84 ± 1.19 µm at 3 months, while cell length increased from 9.57 ± 1.36 µm to 12.05 ± 1.69 µm, respectively. As the thallus cells enlarged during the 3-month cultivation period, the cell density in *H. durvillei* decreased compared with the density at 0, 1, and 2 months, and this decrease was statistically significant. Cell density decreased from 21 ± 3 at 0 months to 13 ± 2 at 3 months.

Table 1 Outer cortical cell size and cell density observed in the surface view of *H. durvillei* thalli at different cultivation periods (0, 1, 2 and 3 months).

Cultivation period (Month)	Cell density (# per 1,000 µm^2)	Cell size	
		Width (µm)	Length (µm)
0	21 ± 3 ^{a}	7.38 ± 1.06 ^{d}	9.57 ± 1.36 ^{d}
1	17 ± 3 ^{b}	8.14 ± 1.48 ^{c}	10.04 ± 2.08 ^{c}
2	16 ± 1 ^{c}	8.47 ± 1.36 ^{b}	10.92 ± 1.50 ^{b}
3	13 ± 2 ^{d}	9.84 ± 1.19 ^{a}	12.05 ± 1.69 ^{a}

Note: Values followed by the same lowercase letters within a column (a, b, c, d) are not significantly different according to Duncan's multiple range test ($p < 0.05$); n = 400 for cell size; n = 40 for the cell density.

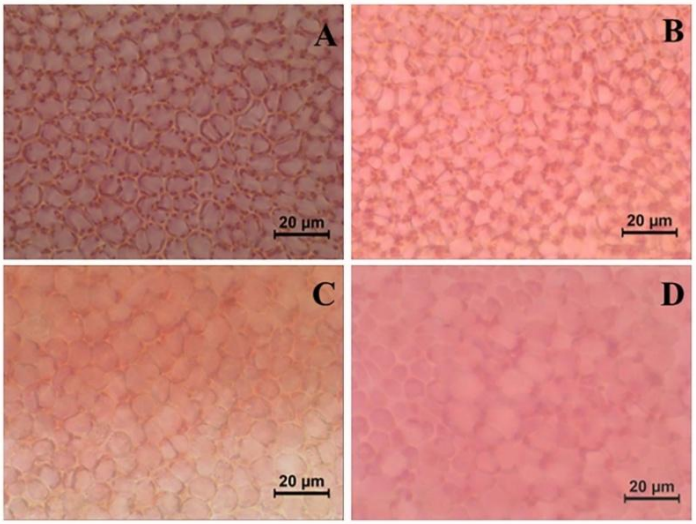


Figure 4 Light micrographs of outer cortical cells of *H. durvillei* thalli at different cultivation periods: (A) initial stage (0 month), (B) 1 month, (C) 2 months, and (D) 3 months.

The transverse section of the *H. durvillei* thallus revealed 3 distinct anatomical layers (**Figures 5(A) - 5(E)**). The outer cortex, forming the outermost region of the thallus, consisted of 1 - 2 layers of vertically elongated cortical cells arranged in a rabbit ear-like pattern. Beneath this layer, the inner cortex consisted of 2 - 4 layers of elongated polygonal cells oriented parallel to the thallus surface and containing visible pigments. The center region of the thallus comprises the medulla, which was formed by filamentous cells interconnected into a continuous network. In addition, large gland cells were occasionally observed interspersed within the medulla region. The overall anatomical organization of the thallus remained consistent across all cultivation periods. However, overall thallus thickness increased with increasing cultivation periods, as summarized in **Table 2**. The mean thallus thickness increased from 340.73 ± 87.04 µm at 0 months to 388.22 ± 83.49 µm, 469.77 ± 107.07 µm, and 558.10 ± 130.27 µm at 1, 2, and 3 months, respectively. All cultivation periods differed significantly from one another according to Duncan's multiple range test ($p < 0.05$).

Table 2 Thallus thickness of *H. durvillei* thallus at different cultivation periods (0, 1, 2, and 3 months).

Cultivation period (months)	**Thallus thickness (µm) N = 120**
0	340.73 ± 87.04 ^{d}
1	388.22 ± 83.49 ^{c}
2	469.77 ± 107.07 ^{b}
3	558.10 ± 130.27 ^{a}

Note: Values followed by the same lowercase letters within a column (a, b, c, d) are not significantly different according to Duncan's multiple range test ($p < 0.05$); n = 120 for the thallus thickness.

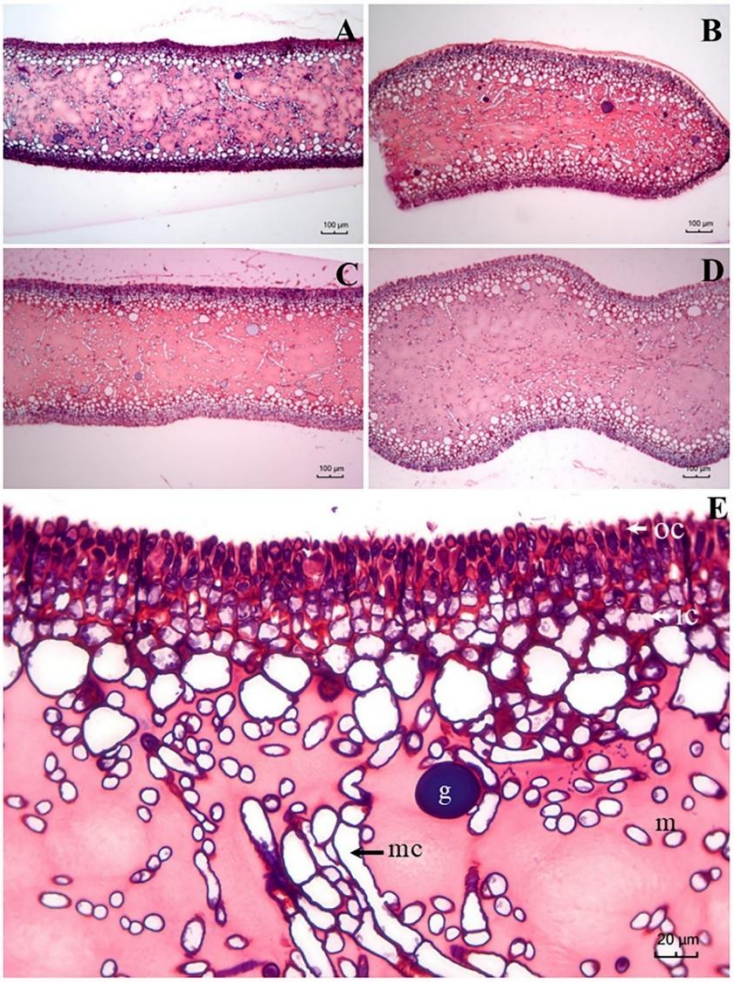


Figure 5 Anatomical characteristics of *H. durvillei* thalli at different cultivation periods: (A) initial stage (0 month), (B) 1 month, (C) 2 months (D) 3 months, and (E) higher magnification of the initial stage (0 month), Abbreviations: (g) grand cell; (ic) inner cortex; (m) medulla; (mc) medulla cell; (oc) outer cortex.

The ultrastructure of *H. durvillei* cells revealed a cell wall composed of cellulose fibrils, with adjacent cells interconnected by a middle lamella (**Figure 6(A)**), within which pit plugs were present. The pit plug was a short cylindrical structure of a dome-shaped outer wall, consisting of an outer cap membrane and an inner region containing protein deposits (**Figure 6(B)**). Immediately beneath the cell wall lies the plasma membrane (**Figure 6(A)**), a thin membrane enclosing the protoplasm. At this layer, plasma membrane-associated vesicles were observed adjacent to the plasma membrane, appearing as vesicular protrusions extending into the cytoplasm (**Figure 6(C)**). The protoplasm consisted of the nucleus and cytoplasm. Within the cytoplasm, large stellate chloroplasts were observed (**Figure 6(D)**). These chloroplasts contained parallel thylakoids bearing phycobilisomes (**Figure 6(E)**), as well as a pyrenoid characterized by a proteinaceous core surrounded by a starch sheath (**Figure 6(G)**). Floridean starch granules, which were frequently observed in close association with the chloroplasts (**Figure 6(F)**). In addition, spherical plastoglobules were observed within the chloroplasts. In the cytoplasm outside the chloroplast, lipid droplets accumulated in the cell, along with additional floridean starch granules (**Figure 6(F)**).

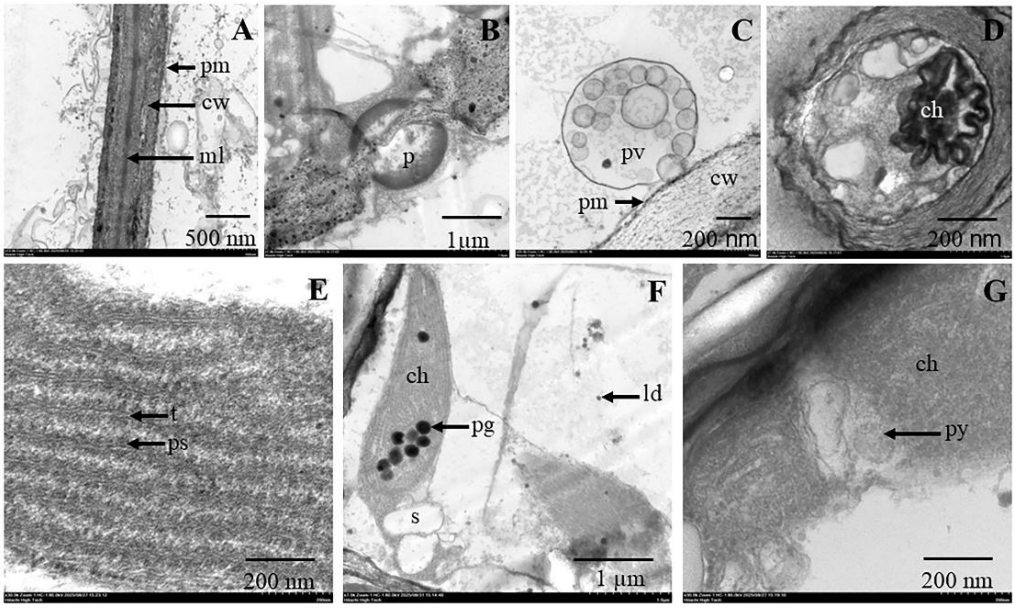


Figure 6 Ultrastructural features of *H. durvillei* thallus cells. (A) Cell wall with adjacent cells connected by the middle lamella. (B) Pit plug in the cell wall. (C) Plasma membrane-associated vesicles. (D) Stellate chloroplast in the cell of the thallus. (E) Filamentous thylakoids with phycobilisomes attached to their surface inside the chloroplast. (F) Floridean starch granules and lipid droplets are distributed within the cytoplasm, whereas plastoglobules are observed within the chloroplast. (G) Pyrenoid in a chloroplast. Abbreviations: ch = chloroplast; cm = cell membrane; cw = cell wall; pv = plasma membrane-associated vesicles; ld = lipid droplet; m = mitochondria; ml = middle lamella; n = nucleus; p = pit plug; pg = plastoglobuli; ps = phycobilisome; py = pyrenoid; s = floridean starch; t = thylakoid.lomal.

Observations of cellular structural changes with increasing culture period revealed progressive alterations in intracellular organization. Thallus cell enlargement was observed after 1 month of cultivation, followed by cell division at 2 months, and continued growth and development, leading to cellular maturity at 3 months. At the initial stage of cultivation, algal cells exhibited well-preserved structural integrity, identified by large chloroplasts containing plastoglobules, with floridean starch granules present in the cytoplasm and frequently observed adjacent to the chloroplasts. In addition, numerous lipid droplets were observed within the cytoplasm (**Figure 7(A)**). After one month of cultivation, the intracellular organization began to change, as evidenced by a reduction in floridean starch granules and lipid accumulation, accompanied by an increase in cell wall thickness (**Figure 7(B)**). After 2 months of cultivation, an increase in chloroplast area was observed, together with renewed accumulation of lipids within the chloroplasts and floridean starch granules in the cytoplasm (**Figure 7(C)**). After 3 months of cultivation, algal cells again exhibited well-preserved cellular integrity, with more pronounced accumulation of lipids within the chloroplasts, as well as numerous lipid droplets and floridean starch granules in the cytoplasm (**Figure 7(D)**). These ultrastructural features suggested enhanced intracellular storage and structural reorganization during prolonged cultivation. Consistently, TEM observations showed an increased accumulation of storage compounds, including floridean starch granules in cytoplasm (**Figures 8(A) - 8(D)**) and plastoglobuli within chloroplasts (**Figures 9(A) - 9(D)**). Overall, a general tendency toward increased accumulation of floridean starch and lipid droplets with cultivation time was observed.

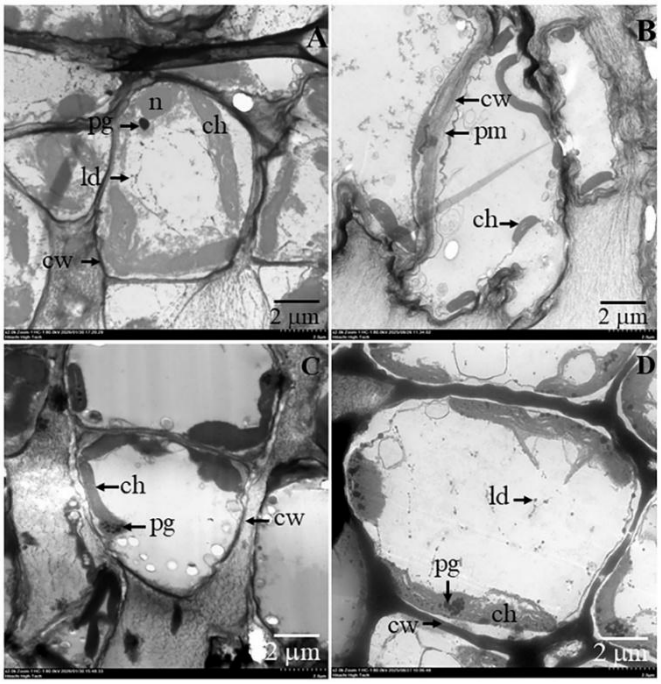


Figure 7 TEM micrographs showing the ultrastructure of thallus cells of *H. durvillei* at different cultivation periods: (A) initial stage, (B) after 1 month of cultivation, (C) after 2 months of cultivation, and (D) after 3 months of cultivation. Scale bars = 2 µm. ch = chloroplast, cm = cell membrane, cw = cell wall, ld = lipid droplet, ml = middle lamella, n = nucleus, pg = plastoglobuli.

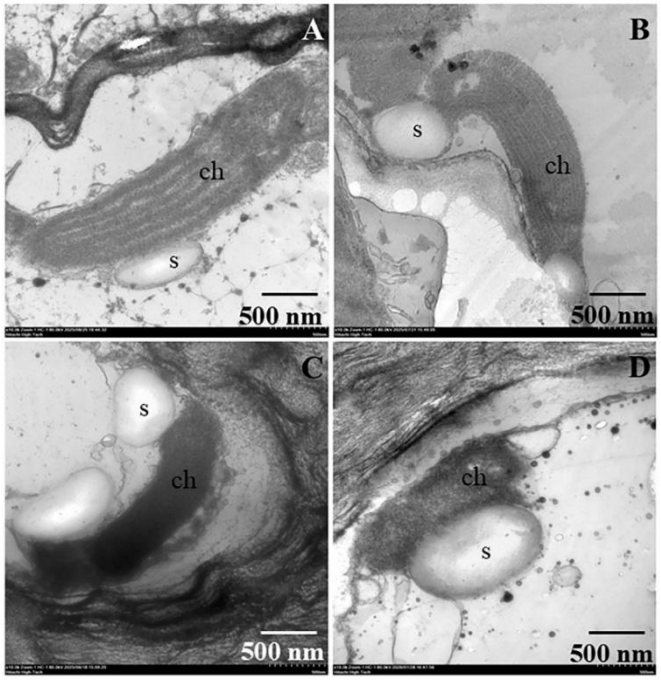


Figure 8 TEM micrographs of *H. durvillei* showing chloroplast-containing cytoplasm and associated floridean starch granules at different cultivation stages. Panels (A-D) demonstrate a progressive increase in the size of floridean starch granules. Scale bars: (A, B, C, D) = 500 nm. Ch = chloroplast, s = floridean starch granule.

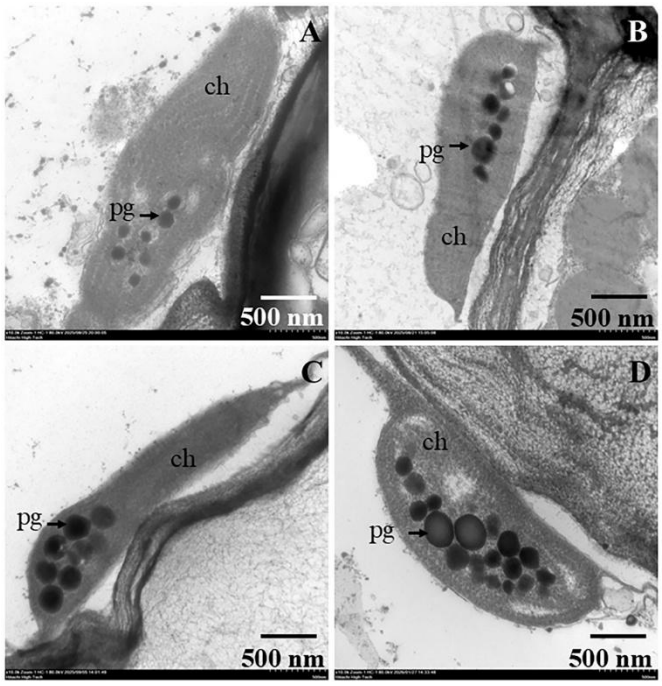


Figure 9 TEM micrographs of chloroplasts in *H. durvillei* showing plastoglobule at different cultivation stages. Panels (A-D) demonstrate a progressive increase in the size and number of plastoglobule granules. ch = chloroplast, pg = plastoglobuli.

This study demonstrates that morphological and anatomical modifications in *H. durvillei* thalli are strongly influenced by cultivation duration, allowing the identification of an optimal harvest time at approximately 3 months. At this stage, thalli were thickest, indicating advanced structural growth and development. A similar trend has been reported in other red algae, where extended growth periods promote cell enlargement [35]. The thallus thickness observed in this study was within the range previously reported for *H. durvillei* from South Africa (450 - 1,000 μm) [33]. Outer cortical cell enlargement was identified as one of the factors contributing to thallus thickening, with a progressive increase in cell diameter over time, indicating that cellular expansion is closely linked to thallus maturation.

Such cell enlargement in *H. durvillei* was associated with increased metabolic activity and enhanced photosynthetic capacity, consistent with general observations reported for algae [6]. In red algae, cells in the cortical layer contained abundant pigments, whereas the central region of the thallus comprised the medullary layer, in which cells formed interwoven filamentous structures [36].

However, the growth of red algal cells is regulated by multiple interacting factors that influence both cell division and cell enlargement, including light, temperature, salinity, nutrients, and water motion [14,16,35,37,38]. In addition to these environmental drivers, sufficient cultivation time is essential to allow progressive cellular growth and tissue development. In the present study, the progressive enlargement of outer cortical cells during prolonged cultivation appears to be a key contributor to thallus thickening, with cortical cell diameters increasing progressively during the 3-month cultivation period. These results indicate that cellular expansion is closely linked to thallus maturation in *H. durvillei*. This structural framework provides the physical context for cellular expansion and organelle development within the thallus.

The structural characteristics of red algal cell walls observed in the present study are consistent with previous reports that describe cellulose microfibrils embedded within a matrix of complex polysaccharides, including agar and carrageenan [39]. In Rhodophyta, the cell wall is composed of cellulose microfibrils integrated into a carbohydrate matrix predominantly consisting of sulfated galactans—such as agar (agarose and agaropectin) and carrageenan—along with

hemicelluloses including glucomannan and sulfated mixed-linkage glucans (MLG) [40]. Red algal cell walls are also rich in sulfated polysaccharides, particularly sulfated galactans, as well as mannan polymers associated with cellulose or glucomannan fibrils [41]. The well-developed cell wall observed in this study provides a structural framework that supports cellular expansion and internal organelle differentiation within the thallus. Such structural reinforcement is essential for maintaining tissue organization during growth and maturation. In addition, pit plugs were clearly identified between adjacent cells. In red algae, pit plugs originate from incomplete cytokinesis, during which partial cell wall formation leaves an intercellular opening that is subsequently sealed by the deposition of a proteinaceous plug [36]. These structures are regarded as a diagnostic ultrastructural feature of Rhodophyta and contribute to mechanical stability and controlled intercellular continuity within the thallus. Collectively, these structural characteristics establish the physical context necessary for chloroplast enlargement and the accumulation of photosynthetic storage products observed at later cultivation periods.

In addition, vesicles were observed adjacent to the plasma membrane in thallus cells of *H. durvillei*, suggesting active vesicle trafficking during cultivation. Their presence may be associated with localized cell wall deposition, considering of the observed increase in cell wall thickness over time. A comparable spatial relationship between vesicle exocytosis and cell wall growth has been reported in the red alga *Antithamnion nipponicum*, where vesicle secretion was restricted to specific growth bands along the cell wall [42]. Consistent with these findings, structural studies in walled organisms, including plant systems such as Arabidopsis thaliana, have demonstrated that cell wall biogenesis is mediated by vesicle trafficking and exocytosis. These processes may occur through localized or polarized secretion mechanisms [43]. Although the biochemical composition of the observed vesicles was not determined in the present study, these observations collectively suggested that vesicle-mediated processes might be involved in cell wall deposition during thallus development. However, further molecular or biochemical analyses would be required to confirm this mechanism.

Based on TEM observation in the present study, *H. durvillei* thallus cells contained a single large chloroplast; therefore, increases in cell size during prolonged cultivation periods could not be compensated for by an increase in chloroplast number. In this context, enhanced light-harvesting capacity in *H. durvillei* is likely achieved through chloroplast enlargement and morphological modification, consistent with the scaling concept proposed for photosynthetic cells [44]. The stellate chloroplast morphology is characterized by elongated arms extending toward the cell periphery. This structure increased the surface area available for light absorption and enhanced the spatial interface between the chloroplast and incoming light during extended culture periods [35,44]. Consequently, increases in cell size with longer culture periods may provide additional intracellular space, facilitate chloroplast expansion, and improve light-harvesting efficiency. These chloroplast-level adaptations are therefore expected to directly influence the performance of photosynthetic pigments in red algal cells. Such structural optimization of chloroplast architecture is functionally significant, as it supports the cooperative action of photosynthetic pigments within the phycobilisome antenna complex. Chloroplasts in red algae (Rhodophyta) exhibit considerable morphological diversity and ultrastructural specialization. They have been reported to display stellate, discoid, or lobed morphologies, with phycobilisomes systematically arranged along the thylakoid membranes to maximize light capture under variable irradiance conditions [45,46]. At the ultrastructural level, red algal chloroplasts are characterized by thylakoid membranes bearing phycobilisomes on their stromal surfaces. Chlorophyll *a* is the sole chlorophyll present in these thylakoid membranes, occurring together with carotenoids such as β-carotene and lutein. Chloroplast DNA occurs as multiple nucleoids distributed throughout the stroma, and pyrenoids are also commonly observed within the chloroplast matrix [47]. Functionally, allophycocyanin (APC), phycocyanin (PC), phycoerythrin (PE), and chlorophyll *a* (Chl *a*) act synergistically to enhance light-harvesting efficiency and facilitate effective energy transfer to the reaction centers, particularly under low-light conditions [48]. Beyond their central role in photosynthesis, these pigments also contribute to algal growth and represent

high-value bioactive compounds with recognized antioxidant properties [14]. Moreover, phycobiliproteins have been widely developed for particular purposes, including fluorescent markers and natural colorants [49].

In the chloroplast, the increased abundance and size of plastoglobules observed after 3 months of cultivation, together with the accumulation of floridean starch granules in the cytoplasm, may indicate enhanced storage of both lipids and carbohydrates as thalli progress toward structural maturity. Plastoglobules are recognized as dynamic lipid-containing structures within plastids, serving as reservoirs for lipids, carotenoids, plastoglobulin/fibrillin proteins, and multiple enzymes involved in tocopherol biosynthesis. Rather than being inert lipid droplets, they act as central hubs of plastid metabolism, contributing to mitigating oxidative stress and supporting plastid development and differentiation. Their size and abundance are highly plastic and responsive to environmental conditions [50]. Consistent with their proposed role in plastid differentiation and functional specialization [51], the plastoglobule enrichment observed in *H. durvillei* may therefore reflect advanced plastid maturation and increased lipid storage capacity during thallus development.

Plastoglobules are physically associated with the thylakoid membranes and are involved in lipid metabolism and biosynthetic processes within chloroplasts [52]. In red algae, plastoglobule abundance has been described as electron-dense lipid droplets located within the chloroplast stroma and positioned between thylakoid membranes. Their primary function is lipid storage structures. Plastoglobules are lipid-containing particles located in the chloroplast stroma and positioned between thylakoid membranes. Their primary function is associated with lipid storage. An increase in plastoglobule abundance has been reported in algae under environmental stress conditions, such as exposure to ultraviolet radiation or cadmium [45]. Similar increases in lipid accumulation under environmental stress conditions, particularly nitrogen limitation and temperature variation, have been reported in microalgae [53]. In the present study, however, the algae were cultivated under natural culture conditions without intentional stress treatments. Therefore, the occurrence of plastoglobules may be related to normal metabolic processes or cellular development during the cultivation period rather than stress responses.

Pyrenoids are subchloroplastic structures enriched in the carbon-fixing enzyme Rubisco and constitute key components of the carbon-concentrating mechanism in many algae. They facilitate efficient carbon fixation, particularly under low-CO_2 availability. The presence and structural prominence of pyrenoids observed in the present study may, therefore, indicate an enhanced capacity for carbon assimilation as the thalli develop toward structural maturity [54].

In addition to chloroplast-associated storage, reserve materials in red algal cells are accumulated in the form of floridean starch granules and lipid droplets located within the cytoplasm [55]. Beyond intracellular and plastid-level adaptations, a structural organization at the tissue level also contributes to thallus function; red algae possess a cortex layer composed of pigment-rich cells. The central region of the thallus consists of a medulla of interwoven filamentous cells, within which colorless filaments are present [36]. In addition, gland cells or vesicle cells function in the release of allelopathic compounds that protect against microbial attack and grazing by herbivores. Together, these structural and biochemical features support growth, defense, and photosynthetic performance in the thalli of red algae.

The thickness of the medullary layer of *H. durvellei* increased significantly with cultivation period, reflecting continued anatomical differentiation of the thallus. This layer consisted of a gelatinous matrix interspersed with filamentous cells and occasional gland cells, which are characteristic features of advanced thallus organization in many red algae. This contributed to mechanical stability and nutrient storage [6,36,56]. Gland cells, also referred to as vesicle cells, are involved in the secretion of allelopathic compounds, acting as chemical defense against microbial invasion and grazing pressure [36]. In red algae, starch is accumulated outside plastids in the form of floridean starch granules [57]. Carbon assimilated by algae through photosynthesis is stored as floridean starch [6]. In microalgae, lipid accumulation is known to increase under environmental stress or nutrient limitation [58]. In the present study, intercellular storage materials were observed as floridean starch granules and lipid droplets, indicating active carbon allocation during cultivation. Prolonged

cultivation induced pronounced ultrastructural modifications, including an increased size and abundance of floridean starch granules and plastoglobules. These changes were associated with chloroplast development and cellular enlargement, reflecting enhanced formation of the intercellular storage compartment at the subcellular level. In red algae, floridean starch serves as the primary carbon reserve in the cytoplasm, while plastoglobules are lipid-containing structures within plastids involved in lipid metabolism and storage.

Collectively, these structural and ultrastructural features indicate that a cultivation period of approximately 3 months represents a critical developmental stage for structural maturation and pigment accumulation. This stage is therefore optimal for commercial harvesting and holds significant potential for applications in aquaculture and marine biotechnology. In addition, the cultivated algae exhibit promising potential for biofuel applications, such as lipid extraction and bioethanol production [59,60]. It also could function as an effective carbon sink. This highlights their dual role in sustainable biomass production and carbon sequestration. The research team intends to conduct further chemical analyses to determine optimal cultivation periods for maximizing the yield of valuable bioactive compounds, particularly phycobiliproteins derived from phycobilisomes (specialized light-harvesting complexes), including phycoerythrin, phycocyanin, and phycobilins.

Conclusions

Molecular identification based on *rbcL* gene sequencing confirmed the taxonomic identity of the studied alga. The *rbcL* sequence showed 99% similarity to *H. durvillei* (GenBank accession no. LT969719), and phylogenetic analysis, including ten closely related taxa, further supported that the specimen analyzed in this study belongs to *H. durvillei*. This study demonstrates that the cultivation period has a significant influence on the ultrastructural organization of *H. durvillei*. Thalli cultivated for 3 months exhibited enhanced chloroplast development, an increased abundance of plastoglobules, and a greater accumulation of floridean starch granules in the cytoplasm, indicating advanced plastid maturation and an elevated storage capacity. These structural modifications reflect progressive cellular differentiation and structural optimization of the thallus during prolonged cultivation. The findings provide valuable insights into the cellular basis of thallus development and contribute to determining an optimal harvest time for maximizing biomass quality and biochemical potential

Acknowledgements

This research was financially supported by the Kasetsart University Research and Development Institute (KURDI), Thailand FF (KU) 23.68. and We are grateful to Prof. Dr. S. Seraphin for the fruitful discussion on manuscript preparation.

Declaration of generative AI in scientific writing

During the preparation of this manuscript, the authors used Grammarly (https://www.grammarly.com/) and ChatGPT to check and improve grammar, spelling, punctuation, and language clarity. After using these tools, the authors carefully reviewed and edited the content and took full responsibility for the final version of the manuscript.

CRediT Author Statement

Yupadee Paopun: Conceptualization; Methodology; Investigation; Writing - Original draft; Funding acquisition. **Siriphan Sukkhaeng**: Formal analysis; Software. **Piyanan Thanomchat**: Visualization; Validation; Investigation. **Nustsaba Kronburee**: Investigation. **Chanram Roopkham**: Investigation. **Yanisa Detpakdee**: Investigation. **Nuttha Sanevas**: Investigation. **Prapat Kosawatpat**: Resources. **Naratorn Chumnum**: Resources.

References

[1] JS Zaneveld. The utilization of marine algae in tropical South and East Asia. *Economic Botany* 1959; **13(2)**, 89-131.

[2] EE Mon. The morphology and distribution of *Halymenia durvillei* Bory de Saint-Vincent (Halymeniales, Rhodophyta) from Myanmar. *Journal of Aquatic Science and Marine Biology* 2018; **1(4)**, 15-25.

[3] ADR N'Yeurt. Marine algae from the Suva lagoon and reef, Fiji. *Australian Systematic Botany* 2001; **14(5)**, 689-869.

[4] G de Smedt, O de Clerck, F Leliaert, E Coppejans and LM Liao. Morphology and systematics of the genus *Halymenia* C. Agardh (Halymeniales, Rhodophyta) in the Philippines. *Nova Hedwigia* 2001; **73(3-4)**, 293-322.

[5] S Kawaguchi, S Shimada, T Abe and R Terada. Morphological and molecular phylogenetic studies of a red alga, *Halymenia durvillei*, (Halymeniaceae, Halymeniales) from Indo-Pacific. *Coastal Marine Sciences* 2006; **30(1)**, 201-208.

[6] RE Lee. *Phycology*. Cambridge University Press, New York, 2008, p. 16-93.

[7] DE Schindel and SE Miller. DNA barcoding a useful tool for taxonomists. *Nature* 2005; **435(7038)**, 17.

[8] BE Clarkston and GW Saunders. A comparison of two DNA barcode markers for species discrimination in the red algal family Kallymeniaceae (Gigartinales, Florideophyceae), with a description of *Euthora timburtonii* sp. nov. *Botany* 2010; **88(2)**, 119-131.

[9] DW Freshwater and J Rueness. Phylogenetic relationships of some European *Gelidium* (Gelidiales, Rhodophyta) species, based on *rbc*L nucleotide sequence analysis. *Phycologia* 1994; **33(3)**, 187-194.

[10] B Gavio and S Fredericq. *Grateloupia turuturu* (Halymeniaceae, Rhodophyta) is the correct name of the non-native species in the Atlantic known as *Grateloupia doryphora*. *European Journal of Phycology* 2002; **37(3)**, 349-359.

[11] MS Kim, SY Kim and W Nelson. *Symphyocladia lithophila* sp. nov. (Rhodomelaceae, Ceramiales), a new Korean red algal species based on morphology and *rbc*L sequences. *Botanica Marina* 2010; **53(3)**, 233-241.

[12] AR Sherwood and GG Presting. Universal primers amplify a 23S rDNA plastid marker in eukaryotic algae and cyanobacteria. *Journal of Phycology* 2007; **43(3)**, 605-608.

[13] HW Wang, S Kawaguchi, T Horiguchi and M Masuda. Reinstatement of *Grateloupia catenata* (Rhodophyta, Halymeniaceae) on the basis of morphology and *rbc*L sequences. *Phycologia* 2000; **39(3)**, 228-237.

[14] JL Godínez-Ortega, P Snoeijs, D Robledo, Y Freile-Pelegrín and M Pedersén. Growth and pigment composition in the red alga *Halymenia floresii* cultured under different light qualities. *Journal of Applied Phycology* 2008; **20**, 253-260.

[15] JB Barufi, FL Figueroa and EM Plastino. Effects of light quality on reproduction, growth and pigment content of *Gracilaria birdiae* (Rhodophyta: Gracilariales). *Scientia Marina* 2015; **79(1)**, 15-24.

[16] NAM Rula, ET Ganzon-Fortes, MJR Pante and GC Trono Jr. Influence of light, water motion, and stocking density on the growth and pigment content of *Halymenia durvillei* (Rhodophyceae) under laboratory conditions. *Journal of Applied Phycology* 2021; **33**, 2367-2377.

[17] A Balkrishna, U Agarwal, S Shrivastava, S Chaudhary and V Arya. Therapeutic potential and applications of red algae: A comprehensive scientific review. *Phytochemistry Reviews* 2026; **25**, 821-852.

[18] II Osovskaya and EA Krivorotova. Properties of agarose - a polysaccharide from marine red algae. *Fibre Chemistry* 2024; **55(6)**, 369-372.

[19] A Chaiwichien, T Samrit, S Osotprasit, P Kueakhai, P Sobhon, K Meemon, N Niamnont, P Manohong, K Pranweerapaiboon, M Tamtin and N Changklungmoa. Evaluation of toxicity and anti-oxidation activity of the extracts from *Halymenia durvillei*. *Trends in Sciences* 2022; **19(6)**, 3032.

[20] P Vivithanaporn, T Siangcham, V Tanawoot, R Settacomkul, K Pranweerapaiboon, K Meemon, N Niamnont, M Tamtin, P Sobhon and K Sangpairoj. Apoptotic and autophagic cell death effects of the hexane extract of tropical marine algae *Halymenia durvillei* against human glioblastoma cells: *In vitro* and *in silico* studies. *Trends in Sciences* 2024; **21(2)**, 7157.

[21] JJ Doyle and JL Doyle. A rapid DNA isolation procedure for small quantities of fresh leaf tissue. *Phytochemical Bulletin* 1987; **19**, 11-15.

[22] M Johnson, I Zaretskaya, Y Raytselis, Y Merezhuk, S McGinnis and TL Madden. NCBI BLAST: A better web interface. *Nucleic Acids Research* 2008; **36(2)**, W5-W9.

[23] JR Harris. *Electron microscopy in biology: A practical approach*. Oxford University Press, New York, 1991, p. 1-37.

[24] MA Hayat. *Principles and techniques of electron microscopy: Biology applications*. Cambridge University Press, New York, 2000, p. 85-138.

[25] BE Juniper, GC Cox, AJ Gilchrist and PR Williams. *Techniques for plant electron microscopy*. Holywell Press, Oxford, England, 1970, p. 1-19.

[26] DC Pease. *Histological techniques for electron microscopy*. Academic Press, New York, 1964, p. 260-261.

[27] CE McClung. *Handbook of microscopical technique: For workers in animal and plant tissues.* Hoeber, New York, 1950, p. 84-85.

[28] RJV Pulvertaft. McClung's handbook of microscopical technique. *Journal of Clinical Pathology* 1951; **4(4)**, 497.

[29] JJ Bozzola and LD Russell. *Electron microscopy: Principles and techniques for biologists*. Jones & Bartlett Publishers, Boston, 1992, p. 112-114.

[30] M Hoppert and A Holzenburg. *Electron microscope in microbiology*. Bios Scientific Publishers, Oxford, England, 1998, p. 55-57.

[31] Y Paopun, P Thanomchat, C Roopkham, P Umroong, W Pan-Utai, P Satmalee, P Kosawatpat, B Thongdang and M Tamtin. Structural development of marine green alga (*Ulva rigida* C. Agardh, 1823) during cultivation. *Trends in Sciences* 2023; **20(8)**, 6747.

[32] CAA de Azevedo, V Cassano and MC Oliveira. Diversity of branched *Halymenia* (Halymeniales, Rhodophyta) species on the Brazilian coast: Molecular and morphological analyses reveal three new species. *Phycologia* 2016; **55(4)**, 431-444.

[33] JJ Hernandez-Kantun, AR Sherwood, R Riosmena-Rodriguez, JM Huisman and O de Clerck. Branched *Halymenia* species (Halymeniaceae, Rhodophyta) in the Indo-Pacific region, including descriptions of *Halymenia hawaiiana* sp. nov. and *H. tondoana* sp. nov. *European Journal of Phycology* 2012; **47(4)**, 421-432.

[34] YW Sheng, W Zhang, D Zhao and HW Wang. A morphological and molecular assessment of the genus *Sinotubimorpha* (Halymeniaceae, Rhodophyta). *Journal of Systematics and Evolution* 2012; **50(2)**, 146-152.

[35] PS Dixon. *Biology of the rhodophyta*. Oliver & Boyd, Edinburgh, Scotland, 1973, p. 93-110.

[36] LE Graham, JM Graham and LW Wilcox. *Algae*. Benjamin Cummings, San Francisco, 2009, p. 309-324.

[37] S Augyte, NA Sims, K Martin, SV Wychen, B Panczak, H Alt, R Nelson and LML Laurens. Tropical red macroalgae cultivation with a focus on compositional analysis. *Plants* 2023; **12(20)**, 3524.

[38] J Cotas, A Leandro, P Monteiro, D Pacheco, A Figueirinha, AMM Gonçalves, GJ da Silva and L Pereira. Seaweed phenolics: From extraction to applications. *Marine drugs* 2020; **18(8)**, 384.

[39] V Stiger-Pouvreau, N Bourgougnon and E Deslandes. *Carbohydrates from seaweeds*. *In*: J Fleurence and I Levine (Eds.). Seaweed in health and disease prevention. Academic Press, New York, 2016, p. 223-274.

[40] ZA Popper, G Michel, C Hervé, DS Domozych, WGT Willats, MG Tuohy, B Kloareg and DB Stengel. Evolution and diversity of plant cell walls: From algae to flowering plants. *Annual Review of Plant Biology* 2011; **62**, 567-590.

[41] N Ghassemi, A Poulhazan, F Deligey, F Mentink-Vigier, I Marcotte and T Wang. Solid-state NMR investigations of extracellular matrixes and cell walls of algae, bacteria, fungi, and plants. *Chemical Reviews* 2022; **122**, 10036-10086.

[42] I Mine, K Yuasa, M Uesugi, S Sekida and K Okuda. Band growth and localization of vesicle exocytosis in the red alga *Antithamnion nipponicum* (Ceramiales). *European Journal of Phycology* 2011; **46(3)**, 263-270.

[43] J Yang, S Chang, L Li, X Ma, H Han, Z Liu and J Zhu. Structural insights into cell wall-related vesicle secretion with different mechanisms. *Plants* 2026; **15(4)**, 660.

[44] KA Pyke. Plastid division and development. *The Plant Cell* 1999; **11(4)**, 549-556.

[45] ZL Bouzon, C Simioni and EC Schmidt. *The structure and morphology of red algae chloroplasts*. *In*: MF Hohmann-Marriott (Ed.). The Structural Basis of Biological Energy

Generation. Springer, Dordrecht, Netherlands, 2014, p. 295-308.

[46] K Solymosi. Plastid structure, diversification and interconversions I. Algae. *Current Chemical Biology* 2012; **6(3)**, 167-186.

[47] L Barsanti and P Gualtieri. *Algae: Anatomy, biochemistry, and biotechnology*. CRC Press, Boca Raton, 2014, p. 118-122.

[48] AR Grossman, MR Schaefer, GG Chiang and JL Collier. The phycobilisome, a light-harvesting complex responsive to environmental conditions. *Microbiological Reviews* 1993; **57(3)**, 725-749.

[49] S Sekar and M Chandramohan. Phycobiliproteins as a commodity: Trends in applied research, patents and commercialization. *Journal of Applied Phycology* 2008; **20**, 113-136.

[50] H Nacir and C Bréhélin. When proteomics reveals unsuspected roles: The plastoglobule example. *Frontiers in Plant Science* 2013; **4**, 114.

[51] PK Lundquist. Chromoplast differentiation: A central role for plastoglobule lipid droplets comes into focus. *New Phytologist* 2003; **237**, 1483-1485.

[52] JN Lohscheider and CR Bártulos. Plastoglobules in algae: A comprehensive comparative study of the presence of major structural and functional components in complex plastids. *Marine Genomics* 2016; **28**, 127-136.

[53] A Converti, AA Casazza, EY Ortiz, P Perego and MD Borghi. Effect of temperature and nitrogen concentration on the growth and lipid content of *Nannochloropsis oculata* and *Chlorella vulgaris* for biodiesel production. *Chemical Engineering and Processing: Process Intensification* 2009; **48(6)**, 1146-1151.

[54] BM Long, Y Matsuda and JV Moroney. Algal chloroplast pyrenoids: Evidence for convergent evolution. *Proceedings of the National Academy of Sciences* 2024; **121(14)**, e2402546121.

[55] A Wahid and MA Khan. *Viruses bacteria and thalloid organisms*. Higher Education Commission, Islamabad, Pakistan, 2006, p. 72-77.

[56] HC Bold and MJ Wynne. *Introduction to the algae: Structure and reproduction.* Prentice-Hall Inc, New Jersey, 1978, p. 504-505.

[57] R Viola, P Nyvall and M Pedersén. The unique features of starch metabolism in red algae. *Proceedings of the Royal Society B: Biological Sciences* 2001; **268(1474)**, 1417-1422.

[58] Q Hu, M Sommerfeld, E Jarvis, M Ghirardi, M Posewitz, M Seibert and A Darzins. Microalgal triacylglycerols as feedstocks for biofuel production: Perspectives and advances. *The Plant Journal* 2008; **54(4)**, 621-639.

[59] Q Al-Abdallah, BT Nixon and JR Fortwendel. The enzymatic conversion of major algal and cyanobacterial carbohydrates to bioethanol. *Frontiers in Energy Research* 2016; **4**, 36.

[60] T Li, M Gargouri, J Feng, JJ Park, D Gao, C Miao, T Dong, DR Gang and S Chen. Regulation of starch and lipid accumulation in a microalga *Chlorella sorokiniana*. *Bioresource Technology* 2015; **180**, 250-257.